 DOI: 10.1002/masy.201100256

Controlled Thermolysis of Macromolecule-Metal Complexes as a Way for Synthesis of Nanocomposites

Anatoly D. Pomogailo, Gulzhian I. Dzhardimalieva*

Summary: Metal–polymer nanocomposites, which comprise nanoparticles of metals and/or their oxides and carbides uniformly distributed in stabilizing polymer matrices, are obtained through solid-phase polymerization of metal-containing monomers followed by controlled thermolysis of synthesized metal-containing polymers. The composition, structure and properties of nanocomposites obtained were studied using the methods of X-ray diffraction, electron microscopy, IR spectroscopy and DSC-TGA thermal analysis. The main stages and kinetics peculiarities of thermal transformations of metal-containing monomers were estimated. It is shown that nanoparticles present in these systems have a characteristic core–shell structure that comprises a metal-containing core and a surface layer, i.e., a polymer shell.

Keywords: metal-containing monomers; microstructure; nanocomposites; nanoparticles; pyrolysis; solid-phase polymerization; stabilization

Introduction

Interest to metal-containing polymeric nanocomposites is caused by a unique combination of properties of metals nanoparticles, their oxides and chalcogenides, and by mechanical, film-forming and other characteristics of polymers with opportunities of their use as magnetic materials for record and storage of information, as catalysts and sensors, in medicine and biology.[1] Homo- and copolymers of acrylic and methacrylic acids and their salts are widely used for the stabilization of metal-containing dispersions. On the one hand, carboxylated compounds of a monomeric and polymeric structure can be molecular precursors of nanocomposite materials. On the other hand, carboxyl groups of macroligands are efficient stabilizers of nanoparticles; these functions are frequently developed together in one system. Amphiphilic character of carboxylated polymers and copolymers allows not only to encapsulate nanoparticles of metals or to combine them with polymeric and inorganic matrixes or biological objects, but also allows to give such properties as solubility in various mediums, ability to self-organization, etc. to nanoparticles.

In order to obtain a polymer shell, a nanoparticle surface is commonly modified with certain functional groups, which are subsequently used to bind a polymer; in another case, the role of a modifier is played by initiator molecules that are involved in graft polymerization (e.g., metal oxide nanoparticles coated with polymethylmethacrylate shells are produced by this method [2]). For these purposes, they widely use ring-opening polymerization[3] and various methods of living radical polymerization, e.g., ATRP (atom transfer radical polymerization),[4–6] which enable one to design polymer shells with uniform structures and controlled thicknesses. However, many of these methods are multistage and quite laborious.

Our approach to the production of composites containing nanoparticles with

Laboratory of Metallopolymers, Institute of Problems of Chemical Physics Russian Academy of Sciences, ac. Semenev av., 1, Chernogolovka, Moscow Region, 142432, Russia
Fax: +74965227763; E-mail: adpomog@icp.ac.ru

the core–shell structure is advantageous in the combined synthesis of the nanosized metal particles and the stabilizing polymer shells in situ. This approach is based on solid - phase homo- and copolymerization of metal-containing monomers (MCM) followed by controlled thermolysis of resulting metal-containing polymers. This work is devoted to the study of the kinetic peculiarities of thermal transformations of the MCMs, as well as the composition and structure of the metal–polymer nanocomposites obtained.

Experimental Part

Metal–polymer nanocomposites were obtained through the controlled thermolysis of metal-containing monomers, metal acrylates, and acrylamide complexes of metal nitrates under isothermal conditions at 643–1073 K in a self-generated atmosphere as described in.[7] In order to isolate the polymer matrix, the metal-containing component was extracted from the CoAAm-based polymer nanocomposite by the successive treatment with aqueous 6 N HCl and HNO_3 solutions at 293–323 K, and the residual polymer was thoroughly washed with distilled water and dried in vacuum at 313 K.

X-ray powder diffraction was studied with Philips PW 1050 diffractometers using Cu$K\alpha$ radiation ($\lambda = 1.54184$ Å). IR absorption spectra were registered on a Specord 75 IR spectrophotometer in the wave number range of 200–4000 cm^{-1} using samples prepared as KBr pellets. Thermogravimetric (TGA) and differential scanning calorimetric (DSC) analyses were performed in a Thermal Analyzer (STA 409C Luxx) connected with a quadrupole mass spectrometer QMS 403C Aeolos (NETZCSH, Germany), under nitrogen atmosphere at a heating rate of 5 °C/min.

The structure of metal–polymer nanocomposites was studied with a JEOL transmission microscope (100 kV), and a JEM 3010 high-resolution transmission microscope (300 kV). Samples for transmission electron microscopy were prepared as follows: a powder suspension in hexane was applied onto a carbon-coated copper grid and the solvent was dried in air.

Results and Discussions

A study of the kinetics and mechanisms of thermal transformations of MCM showed that their thermolysis is a multistage process that includes three key macro stages: dehydration, polymerization of the dehydrated monomer, and decarboxylation of the metal-containing groups of the resulting polymer to give a metal-containing phase (Scheme 1).[8,9]

Thermal Transformations of Metal-Containing Monomers

According to thermal analysis data, dehydration of the monomeric crystal hydrates, for example, acrylic acid salts, occurs at $T_{exp} = 353$–487 K ($[Fe_3O(CH_2{=}CHOCO)_6 \cdot 3H_2O]OH$, Fe_3OAcr_6), 413–453 K ($Co(CH_2{=}CHCOO)_2 \cdot H_2O$, $CoAcr_2$), 373–473 K ($NiCH_2{=}CHCOO)_2 \cdot H_2O$, $NiAcr_2$), and that of the acrylamide complex $[Co(CH_2{=}CHCONH_2)_4(H_2O)_2](NO_3)_2$ (CoAAm) occurs at 328–362 K. The increase in the temperature of the dehydrated monomer to Texp = 473–573 K induces solid-phase polymerization. In this temperature region, in addition to the insignificant weight loss by the sample (<10 wt. %), slight gas evolution occurs. In the case of metal acrylates, the major gas components are CO_2 and $H_2C{=}CHCOOH$ and HOOCCH=CHCOOH vapors, which condense at room temperature on the reactor walls. Characteristic temperatures of polymerization are ~543 K ($CoAcr_2$), ~563 K ($NiAcr_2$), ~518 K (Fe_3OAcr_6), and 488–518 K ($Co[OOCCH{=}CHCOO] \cdot 2H_2O$, CoMal). The polymerization is accompanied by changes in the IR absorption spectra of the dehydrated monomer, in particular, a decrease in the intensity of the C=C stretching band and convergence of the C=O stretching frequencies, giving

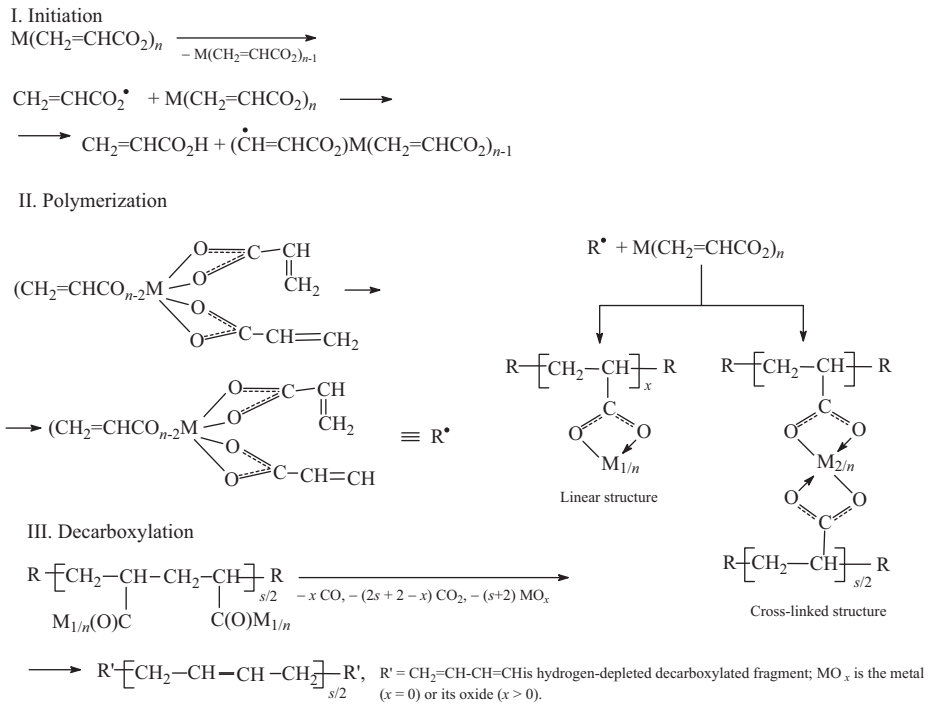

Scheme 1.
The routes of thermal transformations of metal-containing monomers.

rise to one broadened absorption band at 1540–1560 cm^{-1}.

Kinetic Peculiarities of Thermolysis of Metal-Containing Monomers

When $T\exp > 523$ K, thermally polymerized samples undergo intense gas evolution. The gas evolution rate $W = d\eta/dt$ decreases monotonically with an increase of the degree of conversion $\eta = \Delta\alpha_{\sum,t}/\Delta\alpha_{\sum,f}$, where $\Delta\alpha_{\sum,t} = \alpha_{\sum,t} - \alpha_{\sum,0}$, $\Delta\alpha_{\sum,f} = \alpha_{\sum,f} - \alpha_{\sum,0}$, $\alpha_{\sum,f}$, $\alpha_{\sum,t}$, and $\alpha_{\sum,0}$ are the final, current, and the initial numbers of moles of gas products, respectively, evolved per mole of the starting sample at room temperature. The gas evolution kinetics $\eta(\tau)$ is satisfactorily approximated in the general form (up to $\eta \leq 0.95$) by the equation for two parallel reactions:

$$\eta(\tau) = \eta_{1f}[1 - \exp(-k_1\tau)] + (1 - \eta_{1f}) \times [1 - \exp(-k_2\tau)], \quad (1)$$

where $\tau = t - t_0$ (t_0 is the sample heating time, $\eta_{1f} = \eta(\tau)|k_2\tau \to 0$, $k_1\tau \to \infty$, k_1 and k_2 are the effective rate constants for the reactions. The parameters k_1, k_2, η_{1f} and $\Delta\alpha_{\sum,f}$ depend on the temperature of the thermolysis (T_{term}):

$$\eta_{1f}, \Delta\alpha_{\Sigma,f} = A \exp[-E_{a,\,eff}/(RT)], \quad (2)$$

$$k_{eff} = k_{0,\,eff} \exp[-E_{a,\,eff}/(RT)], \quad (3)$$

where A and $k_{0,eff}$ are pre-exponential factors, $E_{a,eff}$ is the effective activation energy.

The initial gas evolution rate $W_{t=0} = W_0$ is

$$W_0 = \eta_{1f}k_1 + (1 - \eta_{1f})k_2. \quad (4)$$

When $k_2 \approx 0$, $\eta_{1f} \to 1$

$$\eta(\tau) \approx 1 - \exp(-k1\tau), \quad (5)$$

$$W_0 \approx k_1. \quad (6)$$

Equations (5) and (6) describe the gas evolution kinetics during thermal transformations of Co(II) acrylate and maleate (Figure 1).

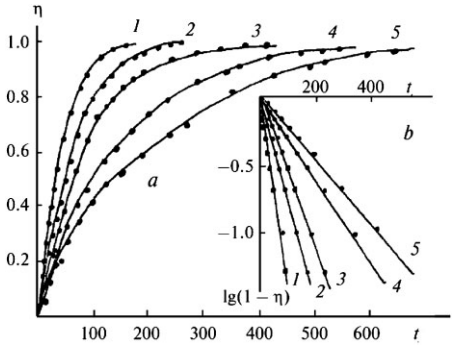

Figure 1.
Gas evolution kinetics $\eta(\tau)$ (*a*) and semilogarithmic lines ($\log(1-\eta)$ *vs.* τ) (*b*) for the thermolysis of Co(II) maleate (CoMal) in self-generated atmosphere at 653 (*1*), 643 (*2*), 633 (*3*), 623 (*4*), and 613 K (*5*).

Composition and Structure of Nanocomposites

The major gaseous product formed in the transformations of the metal acrylates and maleates and their co-crystallizates is CO_2. This was confirmed by IR spectroscopy and mass spectrometry. Carbon monoxide, hydrogen, and H_2O, $H_2C{=}CHCOOH$, and $HOOCH{=}CHCOOH$ vapors, which condense at room temperature, are formed in much smaller amount. Apart from the above-listed gaseous products, CH_4 was found in the case of $CoAcr_2$ (trace amount) and $NiAcr_2$ (amount comparable with CO_2). Electron microscopic examination of the final products of MCM thermolysis showed morphologically similar images, namely, electron-dense particles distributed in a less electron-dense matrix. The particles are nearly spherical, they have a narrow size distribution, and occur as both single structures and aggregates (Figure 2). According to transmission electron microscopy data for the nanocomposite based on Fe(III) acrylate obtained at 663 K (degree of conversion of 55.5%), two fractions of particles with average sizes of 12.3 and 22.1 nm are present. The average size of nanocrystallites calculated by the Scherrer equation is 13.5 nm. According to X-ray diffraction data for the thermolysis product of Co(II) acrylate, the average particle size is 7 nm. The fraction of particles of 6.7 nm size is ~50%, the fractions of 12 and 21 nm

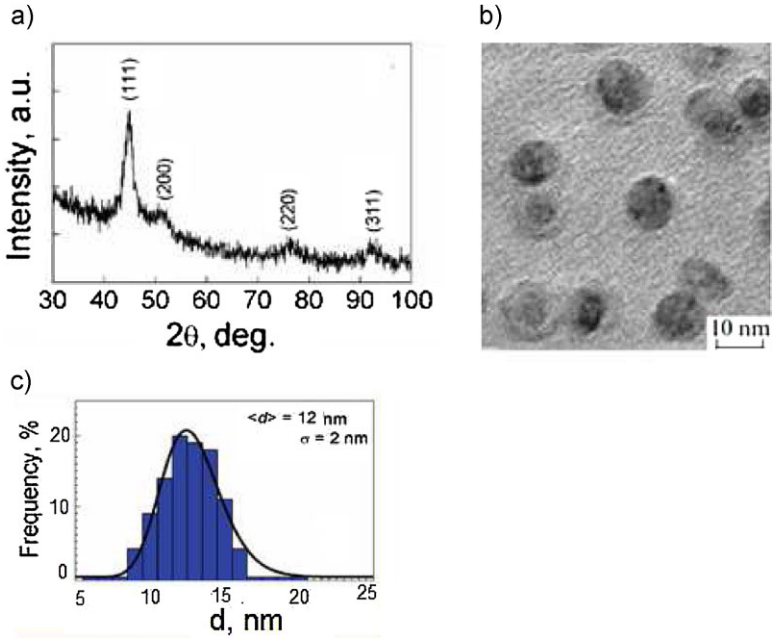

Figure 2.
(a) XRD pattern, (b) micrographs taken with high-resolution electron microscope and (c) nanocrystallite size distribution for thermolysis products of CoAAm ($T_{term} = 643$ K).

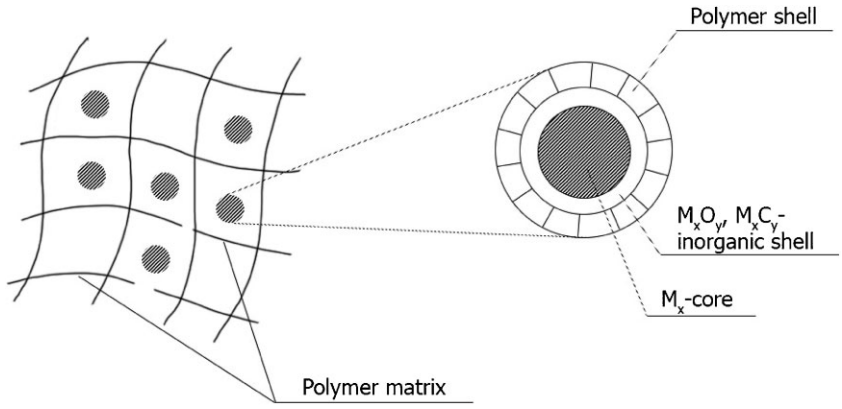

Scheme 2.
The proposed core-shell structure of the nanocomposite.

particles correspond to 27 and 14%, respectively, and the fraction of other particles is 8.4%.

We proposed the core–shell structure of nanoparticles in the synthesized metal nanocomposites which may be schematically represented as follows (Scheme 2):

The sizes and composition of nanoparticles with this structure, as well as the composition of the polymer matrix, depend on the specific type of a metal–polymer composite.

The results of differential scanning calorimetric (DSC) and thermal gravimetric analysis (TGA) of the CoAAm complex are illustrated in Figure 3. TGA-DSC thermograms of the complex were performed under a nitrogen atmosphere. An endo effect assigned to melting is followed by an exo effect related to polymerization about at 373–383 K and 493–523 K (involved all unsaturated ligands of the complex). At higher temperature polymerization is accompanied by a thermal decomposition. TGA curves show three steps of weight losses. One of these (5.9%) is related with elimination of water molecules, including coordinating H_2O. The second step (33.4%) is a thermal degradation which accompanied by chemical reactions of imidization, cyclization, etc. Elimination of H_2O, CO, CO_2, NO, NH_3 at this stage was confirmed by mass-spectra (Figure 3, b). It should be noted that weight loss at the end of thermal transformation is lesser than that can be expected if the product of thermolysis would be a pure metal or metal oxide without pyrolized polymer matrix.

The IR spectra of the initial CoAAm complex are characterized by the presence of absorption bands corresponding to three types of hydrogen bonding, namely, the bonds between amide groups of acrylamide ligands and (3230 cm^{-1}), between an amide group of one AAm ligand and an amide group of another ligand (3300 and 3190 cm^{-1}), and between H_2O and NO_3^- (3390 cm^{-1}) (Table 1).

In the low-frequency spectral region, a broad absorption is observed at 700–500 cm^{-1} with distinctly differentiated maxima at 700, 650, 635, and 586 cm^{-1}, which can be attributed to the large-amplitude slow vibrations of hydrogen-bonded protons. In the spectrum of polymeric CoAAm, the absorption bands remain preserved in the range of the stretching vibrations in OH and NH groups. The absence of the ν(C=C) and δ(=CH) absorption bands at 1580 and 980 cm^{-1} confirms the consumption of C=C bonds as a result of polymerization. In the low-frequency region, the large-amplitude vibrations of protons at 720–520 cm^{-1} also remain preserved. The IR data lead us to conclude that, during the thermolysis, the initial structure of the three-dimensional polymer complex undergoes degradation,

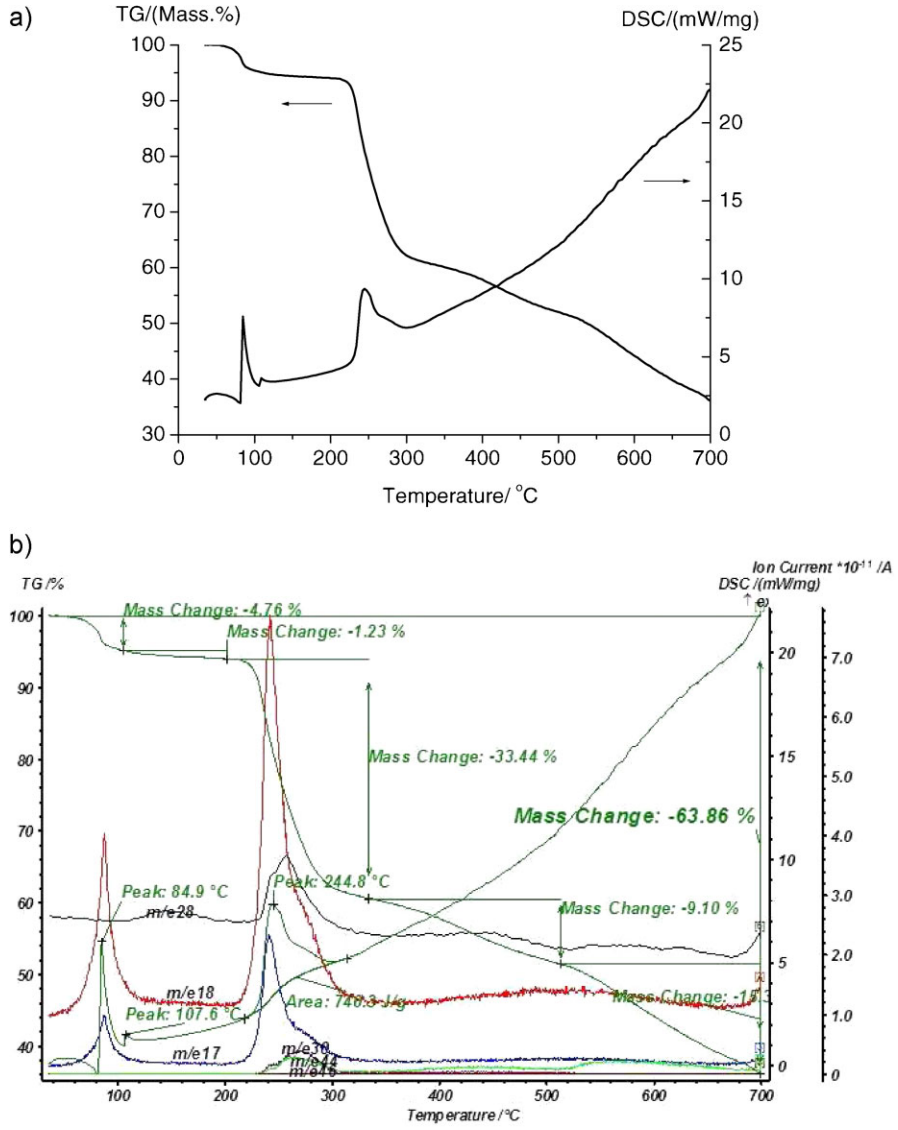

Figure 3.
(a) DSC-TGA curves and (b) DSC-TGA-mass-spectra curves for Co(II)-nitrate acrylamide complex. Heating rate is 5 °C/min.

with some fragments remaining preserved, which is evident from the bands assigned to the stretching vibrations of OH and NH groups (3468 cm^{-1}), out-of-plane deformation vibrations of NH_2 groups (1004 cm^{-1}), and low-frequency vibrations (800, 626 cm^{-1}). Broad absorption bands arise in the region of 1600 cm^{-1}, which attest to the presence of the stretching vibrations of C=C bonds typical of triene and diene conjugated fragments (Figure 4). All of the absorption bands have the Gaussian pattern, which suggests that the interatomic and deformation vibrations occur in a confined space; i.e., the system is characterized by a high degree of crosslinking.

According to the IR and elemental analysis data, the structure of polyconju-

Table 1.
Characteristic frequencies in IR spectra of CoAAm, polymeric CoAAm, product of CoAAm thermolysis at 673 K, and polymer matrix after thermolysis.

Wave number, cm^{-1}					
CoAAm		Poly-CoAAm	product of CoAAm thermolysis at 673 K	polymer matrix after thermolysis	
3390 b.	$\nu asNH_2$	3440 v. b.	3400 v. b.	3425 s. 3200 sh.	
3300 b.	νsNH_2				
2935	$\nu_{as}CH_2$	2925	2925	2930 w.	
2855	ν_sCH_2	2855	2855	2850 w.	
1660	δNH_2		1600	1600 s., b.	ν(C=C)
1380	νNO_3^-	1380 v.n.	1375	1380 n., w. 1330 b.	
980	δ(=CH)	900		905	δNH_2
837	δNH_2		875	770 w.	δCH

Note: abbreviations b., v. b., s., sh., w., n., and v. n. mean broad, very broad, strong, shoulder, weak, narrow, and very narrow, respectively.

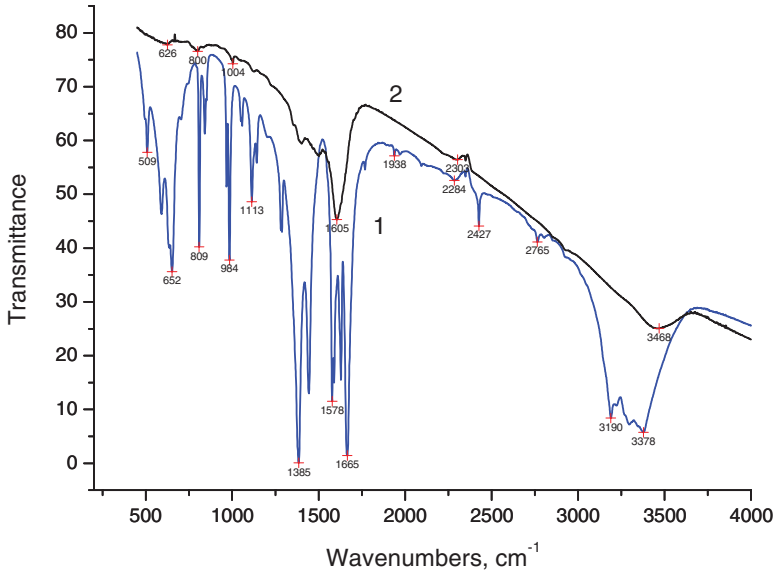

Figure 4.
IR spectra of Co(II) nitrate acrylamide complex (1) and product of CoAAm thermolysis at 673 K.

gated chain units in the thermolysis products of acrylamide complexes may be presented as follows (Scheme 3):

The sizes of metal-containing nanoparticles vary within a range of 5–20 nm depending on the nature of a metal and the thermolysis conditions. According to the data of high-resolution transmission electron microscopy, the thickness of the polymer shell varies in a range of 2–4 to 10–12 nm for different nanocomposites. The metal-containing core may entirely consist of a metal, as, e.g., in the thermolysis products of acrylamide complexes of Co(II) ($T_{term} = 673–873$ K, β-Co with lattice parameter $\alpha_1 = 3.54470$ Å), Ni(II) ($T_{term} = 673–873$ K), and Fe(III) (α-Fe). At higher temperatures of thermolysis, surface layers

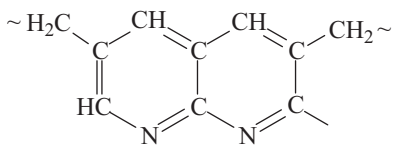

Scheme 3.
The structure of the polyconjugated chain.

(inorganic shells) of corresponding metal carbides are formed around the metal-containing nuclei of the aforementioned nanocomposites (CoCx, $\alpha_2 = 3.61265$ Å for CoAAm ($T_{term} = 1073$ K) and Fe_3C for FeAAm ($T_{term} = 873$ K), with the fraction of these layers being equal to 18–20 wt %). The process of carbide formation can be catalyzed by the metal nanoparticles being formed. On the contrary, in the thermolysis products of metal carboxylates, the metal-containing nuclei contain substantial fractions of inorganic (oxide) shells. For example, upon the thermolysis of Co(II) acrylate, the fraction of CoO in the core is as large as 85%; in the thermolysis of Ni(II) acrylate (wt %): Ni0, ≈ 43; NiO, ≈ 35; and Ni_3C – ≈ 22; while, in the case of the thermolysis of its polymer, Ni_0 ≈ 75 and NiO, ≈ 25. For comparison, let us present the composition of the thermolysis products of Ni(II) polyacrylate, which was prepared via the interaction between polyacrylic acid and Ni(II) acetate, subjected to the thermolysis under the same conditions: [10] Ni ≈ 84 wt % and NiC ≈ 16 wt %.

Conclusion

An analysis of the presented data demonstrates that the thermal transformations of metal-containing monomers give rise to the formation of metal–polymer nanocomposites that contain nanoparticles of metals and/or their oxides and carbides uniformly distributed in stabilizing polymer matrices and have distinct core–shell interfaces. In these systems, nanoparticles are characterized by a specific core–shell structure, which comprises a metal-containing core and a polymer shell as a surface layer. They are distinguished by stability in the course of time; i.e., no changes in the chemical composition, size, and shape of nanoparticles are observed during their long-term storage. It is possible to control the crystallite size, material morphology, fraction of the metal-containing component, and thus the properties by a proper choice of the processing variables. Recently we demonstrated[11] that it was also possible to prepare quasicrystalline intermetallic compounds in the protective matrix in the systems $Al_{65}Cu_{22}Fe_{13}$ and $Al_{54}Cu_9Mg_{37}$ with using the above considered approach. They are formed both earlier and from elements during the formation of a metallopolymer composite material. Three methods of preparation are optimal: from low-dimensional powders of quasicrystals and film-forming polymers, by the *in situ* formation of quasicrystals during the thermal decomposition of the corresponding precursors, and *via* the thermal polymerization of metal-containing monomers (components of quasicrystals) followed by the controlled pyrolysis of the metallopolymers that formed.

Acknowledgements: This work was supported by the Russian Foundation for Basic Research (project no. 11-03-00769) and the Presidium of Russian Academy of Sciences, program no. 24 ''Foundations for Basic Research in Nanotechnologies and Nanomaterials''.

[1] A. D. Pomogailo, V. N. Kestelman, *Metallopolymer nanocomposites*, Springer, Heidelberg **2005**.
[2] D. Holzinger, G. Kickelbick, *J. Mater. Chem.*, **2004**, *14*, 2017.
[3] K. L. Watson, J. Zhu, S. T. Nguen, C. A. Mirkin, *J. Am. Chem. Soc.*, **1999**, *121*, 462.
[4] T. Von Werne, T. E. Patten, *J. Am. Chem. Soc.*, **2001**, *123*, 7497.
[5] A. Kotal, T. K. Mandal, D. R. Walt, *J. Polym. Sci., Part A: Polym. Chem.*, **2005**, *43*, 3631.
[6] S. M. Gravano, R. Dumas, K. Liu, T. E. Patten, *J. Polym. Sci., Part A: Polym. Chem.*, **2005**, *43*, 3675.
[7] E. I. Aleksandrova, G. I. Dzhardimalieva, A. S. Rozenberg, A. D. Pomogailo, *Izv. Akad. Nauk, Ser. Khim.*, **1993**, 1743.
[8] G. I. Dzhardimalieva, *Doctoral Thesis (Chem.)*, Institute of the Problems of Chemical Physics, Russ. Acad. Sci., Chernogolovka **2009**, 399.
[9] A. D. Pomogailo, A. S. Rozenberg, G. I. Dzhardimalieva, *Usp. Khim.*, **2011**, *80*, 272 [*Russ. Chem. Rev.* (*Engl. Transl.*), 2011, 80, 257].
[10] A. S. Rozenberg, G. I. Dzhardimalieva, N. V. Chukanov, A. D. Pomogailo, *Colloid J.*, **2005**, *67*, 51.
[11] S. M. Aldoshin, G. I. Dzhardimalieva, A. D. Pomogailo, Yu. A. Abuzin, *Russ. Chem. Bull., Int. Ed.*, **2011**, *9*, 1837.

